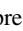


Quenching of oscillations in a liquid metal via attenuated coupling

Ishant Tiwari ^{*}, Richa Phogat ^{*}, Animesh Biswas ^{*}, and P. Parmananda
Department of Physics, Indian Institute of Technology, Bombay, Powai, Mumbai 400076, India

Sudeshna Sinha 

*Department of Physical Sciences, Indian Institute of Science Education and Research Mohali, Knowledge City, SAS Nagar,
 Sector 81, Manauli, P.O. Box 140306, Punjab, India*



(Received 23 January 2022; accepted 23 February 2022; published 14 March 2022)

In this work, we report a quenching of oscillations observed upon coupling two chemomechanical oscillators. Each one of these oscillators consists of a drop of liquid metal submerged in an oxidizing solution. These pseudoidentical oscillators have been shown to exhibit both periodic and aperiodic oscillatory behavior. In the experiments performed on these oscillators, we find that coupling two such oscillators via an attenuated resistive coupling leads the coupled system towards an oscillation quenched state. To further comprehend these experimental observations, we numerically explore and verify the presence of similar oscillation quenching in a model of coupled Hindmarsh-Rose (HR) systems. A linear stability analysis of this HR system reveals that attenuated coupling induces a change in eigenvalues of the relevant Jacobian, leading to stable quenched oscillation states. Additionally, the analysis yields a threshold of attenuation for oscillation quenching that is consistent with the value observed in numerics. So this phenomenon, demonstrated through experiments, as well as simulations and analysis of a model system, suggests a powerful natural mechanism that can potentially suppress periodic and aperiodic oscillations in coupled nonlinear systems.

DOI: [10.1103/PhysRevE.105.L032201](https://doi.org/10.1103/PhysRevE.105.L032201)

I. INTRODUCTION

Scientific literature is replete with examples of oscillating entities in both temporal and spatially [1,2] extended natural and laboratory systems [3–8]. The mercury beating heart (MBH) is a system, wherein both the mechanical movements of the mercury drop and the redox system potential are oscillatory in nature [9,10]. Given appropriate system parameters, this drop of mercury kept in the presence of an oxidizing agent may exhibit both periodic [9] and aperiodic oscillations [11]. The excitatory nature of these chemomechanical oscillations makes this system an ideal tabletop system to demonstrate and verify a plethora of intriguing behaviors observed or predicted in such systems. A few examples are the entrainment [6,12–14], synchronization [15,16], Kuramoto transition [17,18], quorum sensing [19–21], and cessation of oscillations [22–26].

Quenching of oscillation may prove to be both detrimental and advantageous to a system depending on a wide variety of circumstantial factors [27,28]. A sustained rhythmic activity would be a prerequisite for the proper functioning of cardiac cells [29], whereas it would be detrimental to a stable laser output [30]. In the current work, we explore the quenching as well as the revival of oscillations observed in a system of coupled periodic and aperiodic MBH oscillators. Two oscillating drops of mercury are coupled bidirectionally in such a way that each oscillator receives an attenuated copy of the other

oscillator's redox time series. This was done to emulate the signal attenuation over long distances. A robust quenching of oscillations is observed when the attenuation of the signals is above a critical threshold. The experimental observations are numerically corroborated in a system of coupled Hindmarsh-Rose (HR) oscillators [31,32]. The HR oscillators are kept in both periodic and chaotic regimes and coupled to each other in varying degrees of attenuation, to mimic the experimental results involving periodic and aperiodic MBH systems. In addition, linear stability analysis of the HR neurons is performed as a function of the attenuation factor α . This linear stability analysis reveals a stabilization of the system's fixed points when α crosses a critical threshold.

This work is organized in the following manner. In Sec. II, the experimental setup and their corresponding results are presented. These results are followed by numerical simulations corroborating the experiments, using a model system of coupled Hindmarsh-Rose (HR) oscillators in Sec. III. Finally, the results of our work are summarized and discussed in Sec. IV.

II. EXPERIMENTS**A. Experimental setup**

A schematic diagram showing the experimental setup is presented in Fig. 1. It consists of two periodic (aperiodic) oscillators coupled bidirectionally with the help of an operational amplifier. The redox voltage from one MBH (O1) is initially scaled by an attenuation factor α by the first operational amplifier working as an inverting amplifier. The

^{*}These authors contributed equally to this work.

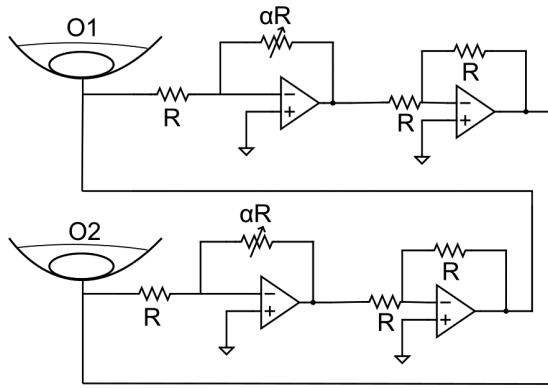


FIG. 1. Experimental setup for bidirectionally coupling two periodic (aperiodic) mercury beating heart oscillators in which an attenuated signal of one oscillator is fed to the other.

attenuated but inverted signal is then passed through another unity gain inverting amplifier and subsequently coupled to the second MBH via a coupling resistor. This circuit is repeated for the second MBH (O2) as well to construct a bidirectional coupling scenario. One can couple the two oscillators with varying degrees of attenuation by controlling the factor α through the variable resistors. The coupling between the two MBH oscillators is initially switched on without any attenuation, i.e., $\alpha = 1$. Subsequently, α is slowly decreased till the oscillations in the two oscillators are quenched. The electrolyte used to immerse the mercury drops was a mixture of 6M H_2SO_4 and 0.2M $\text{Ce}_2(\text{SO}_4)_3$ solutions. A grounded, reducing Fe nail was kept near the drops so as to maintain autonomous oscillations of the drop. The redox time series of the oscillating mercury drop was recorded by immersing a Pt wire into the mercury drop and recording its potential difference with respect to the ground. To generate periodic oscillations, the drops were placed in a container of a small radius of curvature compared to the aperiodic scenario where a much shallower watch glass with a larger radius of curvature was used.

B. Experimental results

Figure 2 shows the system dynamics of two periodic MBH oscillators. At $t \approx 320$ s, the oscillators are bidirectionally coupled to each other without any attenuation in their signals, i.e., $\alpha = 1$. This leads to the dynamics of the two oscillators to be in-phase synchronized with each other. Subsequently, the signal is gradually attenuated by slowly decreasing α from $t \approx 340$ s onward, and the oscillations are quenched at $t \approx 355$ s. After $t \approx 360$ s, the coupling is switched off, due to which the oscillations of the two systems are revived. The three insets in Fig. 2 from left to right show representative zoomed-in dynamics of the initial unsynchronized aperiodic MBH oscillators, the coupled synchronized dynamics when there is no attenuation, and the final uncoupled dynamics after the coupling is switched back off.

In Fig. 3, we present the scenario when two aperiodic MBH oscillators are coupled via the coupling scheme mentioned in Fig. 1. Similar to the periodic MBH case, we find that coupling aperiodic oscillators without any attenuation ($\alpha = 1$)

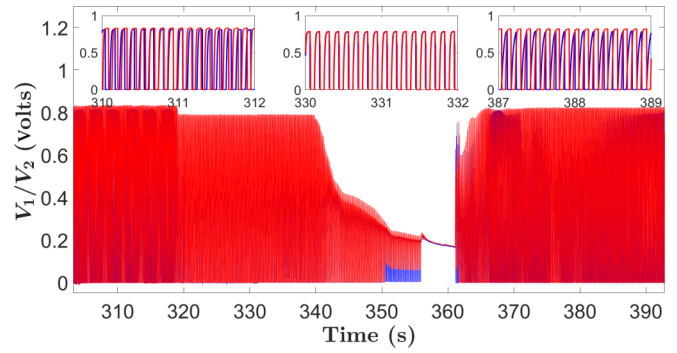


FIG. 2. Dynamics of two periodic MBH systems are displayed in red and blue. Initially the oscillators are uncoupled ($t < 320$ s and left inset). At $t \approx 320$ s, the oscillators are coupled without any signal attenuation and their dynamics become synchronized (middle inset). Following this, the attenuation in the coupling signals is gradually increased from $t \approx 340$ s till the quenching of oscillations at $t \approx 355$ s. This attenuated coupling is switched off at $t \approx 360$ s, after which the two systems resume their autonomous periodic oscillations (right inset).

leads to an emergence of synchronized ($10 \text{ s} \lesssim t \lesssim 40 \text{ s}$) dynamics between the two oscillators. Similar to the periodic scenario, α is gradually decreased for the aperiodic oscillators as well. This leads to a cessation of oscillations being eventually achieved at $t \approx 50$ s. As the coupling is switched off at $t \approx 60$ s, the autonomous aperiodic oscillations of the two systems are reinvigorated. The three insets in Fig. 3 from left to right show representative zoomed-in dynamics of the initial unsynchronized aperiodic MBH oscillators, the coupled synchronized dynamics when there is no attenuation, and the final uncoupled aperiodic dynamics after the coupling is switched back off.

From these experiments, it is evident that, if the coupling between two oscillators is sufficiently attenuating the signal in transit, there is a possibility for the coupled system to go to a

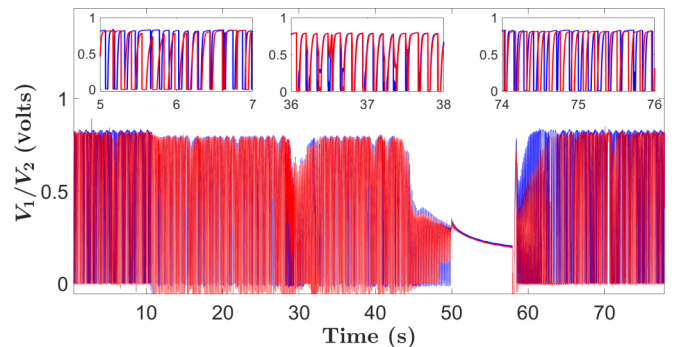


FIG. 3. Dynamics of two aperiodic MBH systems are displayed in red and blue colors. Initially the two aperiodic MBH oscillators are uncoupled ($t \lesssim 10$ s and left inset). The oscillators are coupled without any signal attenuation and their dynamics become synchronized (middle inset) during $10 \text{ s} \lesssim t \lesssim 40 \text{ s}$. Following this, the attenuation in the coupling signals is gradually increased till the quenching of oscillations at $t \approx 50$ s. The coupling is switched off at $t \approx 60$ s after which the two systems resume their autonomous aperiodic oscillations (right inset).

fixed point state. In the next section, we try to understand this phenomenon by recreating these observations in a numerical system of coupled HR oscillators.

III. COUPLED OSCILLATOR MODEL

To numerically corroborate the experimental results in a model system mimicking our experiments, we simulate the HR system. This is a system of three coupled ordinary differential equations [32] and can exhibit relaxation oscillations similar to the ones observed in an MBH oscillator. We took two such HR neurons and coupled them via attractive bidirectional coupling. The system equations for our simulations are as follows:

$$\dot{x}_i = y_i - ax_i^3 + bx_i^2 - z_i + I_i - k(x_i - \alpha x_j), \quad (1)$$

$$\dot{y}_i = c - dx_i^2 - y_i, \quad (2)$$

$$\dot{z}_i = \epsilon [s(x_i - x_i^R) - z_i]. \quad (3)$$

Here, x_i , y_i , and z_i denote the three dynamical variables of the HR system for the i th oscillator where $i = 1$ and 2 . The term $k(x_i - \alpha x_j)$ denotes the coupling between the two oscillators. The incoming signal from the other oscillator is attenuated by a factor α in this term. When $\alpha = 1$, there is no attenuation, while the limiting case of $\alpha \rightarrow 0$ indicates the situation where the signal is so attenuated that the influence of the coupled oscillator approaches zero. So α reflects the strength of the feedback [33] from the other oscillator in the coupling interaction.

The system parameters are kept such that the autonomous systems exhibit either periodic or aperiodic bursting dynamics. The parameters $a = 1$, $b = 3$, $c = 1$, $d = 5$, $s = 4$, $\epsilon = 0.0021$, and $x_i^R = (-8/5)$ are kept constant during all the simulations. The parameters I_1 and I_2 are set at 3.21 and 3.22 for periodic dynamics, and at 3.28 and 3.29 for aperiodic dynamics. The coupling constant is kept fixed at $k = 5$ whenever the oscillators are coupled and at zero when uncoupled. The attenuating parameter α serves as the control parameter that is varied during the simulations to mimic the experiments.

A. Numerical results

In Fig. 4, it is observed that when two periodic HR neurons are coupled to each other without attenuation ($\alpha = 1$ at $t = 4000$), they exhibit synchronized dynamics. As the attenuation is increased (i.e., α is decreased to 0.7 at $t = 7000$), both the systems converge to a fixed point. The oscillations of the two systems are revived when the coupling is switched off at $t = 10000$. The three insets in Fig. 4 from left to right show representative zoomed-in dynamics of the initially unsynchronized oscillators, the coupled synchronized dynamics when there is no attenuation, and the final uncoupled dynamics after the coupling is switched back off.

Figure 5 presents the scenario when two aperiodic HR neurons are coupled. Initially, at $t = 4000$, the two systems are coupled with an attenuation factor of $\alpha = 1$ and the two systems become synchronized with each other. At $t = 7000$, α is decreased to 0.7 and the oscillations of the two systems cease. Autonomous aperiodic oscillations in the two HR neurons are

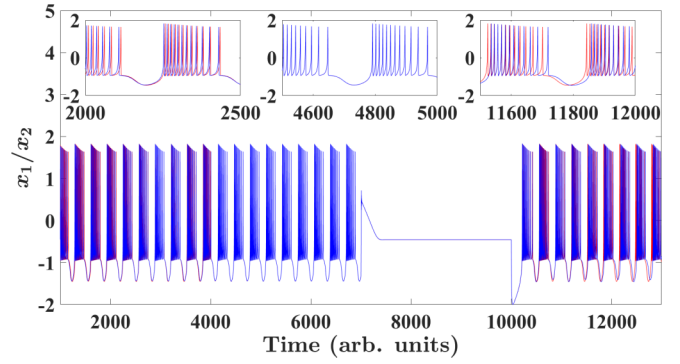


FIG. 4. Dynamics of two periodic HR neurons are displayed in red and blue. Initially the systems are uncoupled ($t < 4000$ s and left inset). The oscillators are coupled without any signal attenuation, i.e., $\alpha = 1$ and their dynamics become synchronized (middle inset) during $4000 < t < 7000$. Following this, the attenuation factor α is decreased to 0.7 at $t = 7000$ and a quenching of oscillations is observed. The coupling is switched off at $t = 10000$, after which the two systems resume their autonomous periodic oscillations (right inset).

revived when the systems are uncoupled at $t = 10000$. The zoomed-in panels of Fig. 5 show the uncoupled dynamics (left), synchronized dynamics (center), and final unsynchronized aperiodic oscillations (right) of the two HR neurons.

B. Linear stability analysis

To further understand the reason for the cessation of oscillations when the attenuation in the coupling is increased, we performed an eigenvalue analysis of the coupled HR oscillators. For this purpose, the Jacobian of the six-dimensional coupled system was evaluated. In Figs. 6(a) and 6(b), we show the variation of the maximum value of the real parts of the eigenvalues of this Jacobian matrix (λ_{\max} , solid orange curve) as a function of the attenuation factor α for the periodic

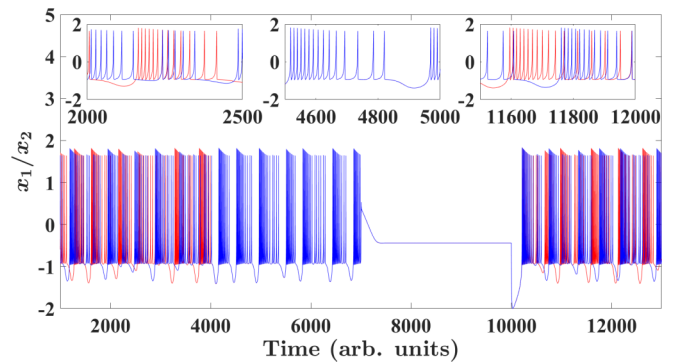


FIG. 5. Dynamics of two aperiodic HR neurons are displayed in red and blue. The systems dynamics for uncoupled aperiodic HR oscillators are shown in the left panel and at $t < 4000$ s. The oscillators are then coupled without any signal attenuation and their dynamics are synchronized (middle inset) during $4000 < t < 7000$. Following this, at $t = 7000$, the attenuation factor α is decreased to 0.7 and the oscillations are quenched. The coupling is switched off at $t = 10000$, after which the two systems resume their autonomous aperiodic oscillations (right inset).

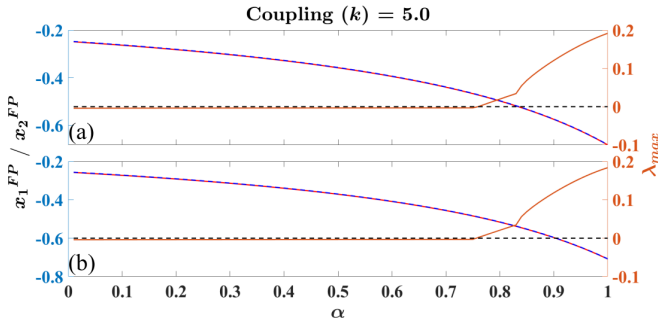


FIG. 6. The dependence of λ_{\max} as a function of α (solid orange curve, right y axis). λ_{\max} crosses the value 0 (dashed black curve) at $\alpha \approx 0.75$. The fixed points of the variables x_1 (red solid curve, left y axis) and x_2 (blue dashed curve, left y axis) as a function of α . The two panels (a) and (b) correspond to the case of periodic and chaotic HR dynamics respectively.

[Fig. 6(a)] and aperiodic [Fig. 6(b)] cases. In both cases, the value of λ_{\max} becomes negative at an α value of around 0.75. That is, there exists a threshold value of attenuation. As the system crosses this value, the fixed point dynamics are stabilized. Additionally, the fixed points of the system variables x_1 and x_2 for the periodic [Fig. 6(a)] and aperiodic [Fig. 6(b)] cases are also plotted as a function of α in red solid and blue dashed curves, respectively. The system converges to these fixed points when α crosses the threshold value from the right. We must also note here that, although the two fixed points x_1^{FP} and x_2^{FP} seem to fall along the same curve in Figs. 6(a) and 6(b), there exists a small difference between their values; i.e., the two variables x_1 and x_2 of the coupled system stabilize to two slightly different values. Since both systems are stabilized to different values, we have an inhomogenous steady state, also known as an oscillation death (OD) state. The fixed point solutions obtained in periodic and aperiodic HR systems, shown in Figs. 6(a) and 6(b), are consistent with the values of the system variable x_i at the time of cessation of oscillations shown in Figs. 4 and 5.

IV. SUMMARY AND DISCUSSION

In this work, we reported the quenching of oscillations in two bidirectionally coupled MBH systems when their individual signals were attenuated before passing on to the other oscillator. This attenuation presented before feeding the signal to the other oscillator is used to mimic a physical situation wherein there is an attenuation of signal amplitude due to various transmission losses. Interestingly, a cessation of oscillations was observed when the signal attenuation crossed a threshold. This cessation was observed for both the periodic and the aperiodic MBH system setups. To understand the experiments, we performed numerical simulations on a coupled Hindmarsh-Rose neuronal model in both periodic and aperiodic domains. Similar to experiments, it was observed that the coupled system ceased to oscillate when the attenuation factor α was below a threshold level. Below this threshold level, it was found that the real part of the maximum eigenvalue of the Jacobian evaluated at the fixed point became negative, indicating the stabilization of fixed point dynamics.

Our results are relevant in settings wherever there are coupled systems separated by space and coupling signals carried over lossy connections. For example, neuronal cells coupled over a large distance may suffer from signal attenuation at the receiver's end. So attenuation-induced oscillation suppression suggests another general mechanism of control of oscillatory behavior in neuronal systems [34,35]. Such attenuation of signals also underpins models of distance-dependent coupling that is believed to be widespread in ecological systems [36]. In summary then, attenuated coupling could potentially lead to the spontaneous stabilization of steady states and indicates another potent natural mechanism for oscillation quenching.

ACKNOWLEDGMENTS

We thank Manoj Aravind from IIT-Bombay for constructive discussions about the design of the electronic circuit used in our experiments.

- [1] P. Parmananda, H. Mahara, T. Amemiya, and T. Yamaguchi, Resonance Induced Pacemakers: A New Class of Organizing Centers for Wave Propagation in Excitable Media, *Phys. Rev. Lett.* **87**, 238302 (2001).
- [2] T. R. Chigwada, P. Parmananda, and K. Showalter, Resonance Pacemakers in Excitable Media, *Phys. Rev. Lett.* **96**, 244101 (2006).
- [3] Y. Kuramoto, *Chemical Oscillations, Waves, and Turbulence* (Springer-Verlag, Berlin, 1984).
- [4] K. Kumar, C. Knie, D. Bléger, M. A. Peletier, H. Friedrich, S. Hecht, D. J. Broer, M. G. Debije, and A. P. Schenning, A chaotic self-oscillating sunlight-driven polymer actuator, *Nat. Commun.* **7**, 1 (2016).
- [5] R. Phogat, S. Sinha, and P. Parmananda, Echo in complex networks, *Phys. Rev. E* **101**, 022216 (2020).
- [6] R. Phogat and P. Parmananda, Provoking predetermined aperiodic patterns in human brainwaves, *Chaos* **28**, 121105 (2018).
- [7] I. Tiwari, P. Parmananda, and R. Chelakkot, Periodic oscillations in a string of camphor infused disks, *Soft Matter* **16**, 10334 (2020).
- [8] R. Phogat, A. Ray, P. Parmananda, and D. Ghosh, Phase coalescence in a population of heterogeneous Kuramoto oscillators, *Chaos* **31**, 041104 (2021).
- [9] G. Lippmann, Beziehungen zwischen den capillaren und elektrischen Erscheinungen, *Annalen der Physik* **225**, 546 (1873).
- [10] D. K. Verma, A. Contractor, and P. Parmananda, Potential-dependent topological modes in the mercury beating heart system, *J. Phys. Chem. A* **117**, 267 (2013).
- [11] P. Kumar and P. Parmananda, Control, synchronization, and enhanced reliability of aperiodic oscillations in the mercury beating heart system, *Chaos* **28**, 045105 (2018).
- [12] I. Bove, S. Boccaletti, J. Bragard, J. Kurths, and H. Mancini, Frequency entrainment of nonautonomous chaotic oscillators, *Phys. Rev. E* **69**, 016208 (2004).

- [13] P. Kumar, P. Parmananda, D. K. Verma, T. Singla, I. de Nicolás, J. Escalona, and M. Rivera, Entrainment of aperiodic and periodic oscillations in the mercury beating heart system using external periodic forcing, *Chaos* **29**, 053112 (2019).
- [14] I. Tiwari, S. Upadhye, V. Akella, and P. Parmananda, Revealing the deterministic components in active avalanche-like dynamics, *Soft Matter* **17**, 2865 (2021).
- [15] D. K. Verma, H. Singh, A. Contractor, and P. Parmananda, Synchronization in autonomous mercury beating heart systems, *J. Phys. Chem. A* **118**, 4647 (2014).
- [16] P. Kumar, D. K. Verma, P. Parmananda, and S. Boccaletti, Experimental evidence of explosive synchronization in mercury beating-heart oscillators, *Phys. Rev. E* **91**, 062909 (2015).
- [17] I. Z. Kiss, Y. Zhai, and J. L. Hudson, Emerging coherence in a population of chemical oscillators, *Science* **296**, 1676 (2002).
- [18] D. K. Verma, H. Singh, P. Parmananda, A. Contractor, and M. Rivera, Kuramoto transition in an ensemble of mercury beating heart systems, *Chaos* **25**, 064609 (2015).
- [19] M. R. Tinsley, A. F. Taylor, Z. Huang, F. Wang, and K. Showalter, Dynamical quorum sensing and synchronization in collections of excitable and oscillatory catalytic particles, *Phys. D (Amsterdam, Neth.)* **239**, 785 (2010).
- [20] D. J. Schwab, A. Baetica, and P. Mehta, Dynamical quorum-sensing in oscillators coupled through an external medium, *Phys. D (Amsterdam, Neth.)* **241**, 1782 (2012).
- [21] H. Singh and P. Parmananda, Quorum sensing via static coupling demonstrated by Chua's circuits, *Phys. Rev. E* **88**, 040903(R) (2013).
- [22] K. Bar-Eli, On the stability of coupled chemical oscillators, *Phys. D (Amsterdam, Neth.)* **14**, 242 (1985).
- [23] R. Phogat, I. Tiwari, P. Kumar, M. Rivera, and P. Parmananda, Cessation of oscillations in a chemo-mechanical oscillator, *Eur. Phys. J. B* **91**, 1 (2018).
- [24] S. S. Chaurasia, M. Yadav, and S. Sinha, Environment-induced symmetry breaking of the oscillation-death state, *Phys. Rev. E* **98**, 032223 (2018).
- [25] A. Biswas, S. Chaurasia, P. Parmananda, and S. Sinha, Asymmetry induced suppression of chaos, *Sci. Rep.* **10**, 1 (2020).
- [26] S. S. Chaurasia, A. Biswas, P. Parmananda, and S. Sinha, Ill-matched timescales in coupled systems can induce oscillation suppression, *Chaos* **31**, 103104 (2021).
- [27] W. Zou, D. Senthilkumar, M. Zhan, and J. Kurths, Quenching, aging, and reviving in coupled dynamical networks, *Phys. Rep.* **931**, 1 (2021).
- [28] A. Koseska, E. Volkov, and J. Kurths, Oscillation quenching mechanisms: Amplitude vs oscillation death, *Phys. Rep.* **531**, 173 (2013).
- [29] J. Miake, E. Marbán, and H. B. Nuss, Biological pacemaker created by gene transfer, *Nature (London)* **419**, 132 (2002).
- [30] A. Prasad, Y.-C. Lai, A. Gavrielides, and V. Kovanis, Amplitude modulation in a pair of time-delay coupled external-cavity semiconductor lasers, *Phys. Lett. A* **318**, 71 (2003).
- [31] J. Hindmarsh and R. Rose, A model of the nerve impulse using two first-order differential equations, *Nature (London)* **296**, 162 (1982).
- [32] J. L. Hindmarsh and R. Rose, A model of neuronal bursting using three coupled first order differential equations, *Proc. R. Soc. London B* **221**, 87 (1984).
- [33] D. Ghosh, T. Banerjee, and J. Kurths, Revival of oscillation from mean-field-induced death: Theory and experiment, *Phys. Rev. E* **92**, 052908 (2015).
- [34] S. Sinha and W. L. Ditto, Controlling neuronal spikes, *Phys. Rev. E* **63**, 056209 (2001).
- [35] M. P. K. Jampa, A. R. Sonawane, P. M. Gade, and S. Sinha, Synchronization in a network of model neurons, *Phys. Rev. E* **75**, 026215 (2007).
- [36] T. Banerjee, P. S. Dutta, A. Zakharova, and E. Schöll, Chimera patterns induced by distance-dependent power-law coupling in ecological networks, *Phys. Rev. E* **94**, 032206 (2016).